PI(4,5)P_2-dependent microdomain assemblies capture microtubules to promote and control leading edge motility

Tamara Golub and Pico Caroni

Friedrich Miescher Institut, Basel, 4058 Switzerland

The lipid second messenger PI(4,5)P_2 modulates actin dynamics, and its local accumulation at plasmalemmal microdomains (rafts) might mediate regulation of protrusive motility. However, how PI(4,5)P_2-rich rafts regulate surface motility is not well understood. Here, we show that upon signals promoting cell surface motility, PI(4,5)P_2 directs the assembly of dynamic raft-rich plasmalemmal patches, which promote and sustain protrusive motility. The accumulation of PI(4,5)P_2 at rafts, together with Cdc42, promotes patch assembly through N-WASP. The patches exhibit locally regulated PI(4,5)P_2 turnover and reduced diffusion-mediated exchange with their environment. Patches capture microtubules (MTs) through patch IQGAP1, to stabilize MTs at the leading edge. Captured MTs in turn deliver PKA to patches to promote patch clustering through further PI(4,5)P_2 accumulation in response to cAMP. Patch clustering restricts, spatially confines, and polarizes protrusive motility. Thus, PI(4,5)P_2-dependent raft-rich patches enhance local signaling for motility, and their assembly into clusters is regulated through captured MTs and PKA, coupling local regulation of motility to cell polarity, and organization.

Introduction

Regulated motility at the cell surface mediates local interactions with the cell environment, cell polarization, and oriented migration processes. Cell responses based on surface motility involve the regulation of actin dynamics (Pollard and Borisy, 2003). In addition, microtubules (MTs) play a decisive role in polarizing motility, and defining the specific positions along the cell surface where motility directs cell organization and behavior (Rodriguez et al., 2003; Gundersen et al., 2004). The sites and mechanisms through which MTs are captured at specific positions along the cell surface are thus of critical importance to organized motility and cell polarity. The lipid second messenger PI(4,5)P_2 is an attractive candidate to integrate signaling and coordinate actin and membrane dynamics in motility. Thus, PI(4,5)P_2 is concentrated at inner leaflet cholesterol-dependent lipid microdomains (rafts), which can accumulate locally to amplify signaling. Furthermore, PI(4,5)P_2 accumulates at sites of cell surface motility, and can modulate both actin dynamics and the assembly of membrane-associated protein coats mediating morphogenesis and membrane trafficking (Botelho et al., 2000; Rozelle et al., 2000; Tall et al., 2000; Martin, 2001; McLaughlin et al., 2002; Yin and Janmey, 2003; Huang et al., 2004). These observations have raised the possibility that protrusive motility at the cell surface may be regulated through the local accumulation of raft domains enriched in PI(4,5)P_2 (Caroni, 2001; Yin and Janmey, 2003). However, whether and how rafts do accumulate locally has remained a controversial issue, and the role of PI(4,5)$_2$-rich rafts in regulating cell surface motility is not clear.

Plasmalemmal rafts are in principle well suited to play major roles in regulating motility at the cell surface (Golub et al., 2004). Thus, among the molecular components involved in actin cytoskeleton regulation, transmembrane proteins associated with rafts include receptor tyrosine kinases and activated integrins, and components associated with inner leaflet rafts include Rho-type GTPases, activated N-WASP, src-like kinases, ERM proteins, PI5-kinase, and PI(4,5)P_2 (Martin, 2001; del Pozo et al., 2004). MT-dependent functions linked to cell surface motility also depend on raft integrity. Thus, (a) raft integrity is critically important to polarize cells (Pierini et al., 2003); (b) chemotacting cells accumulate and require distinct types of rafts and raft-associated signaling components at their leading and trailing edge (Gomez-Mouton et al., 2004); and (c)

Correspondence to P. Caroni: caroni@fmi.ch

Abbreviations used in this paper: dn, dominant-negative; MT, microtubule; PHδ1-GFP, PLCδ1-PH-GFP construct; ppGFP, double-palmitoylated GFP targeting to rafts; ppRFP, double-palmitoylated RFP construct; Rp-cAMPS, membrane-permeable antagonist of cAMP; Sp-cAMPS, membrane-permeable agonist of cAMP.

The online version of this article contains supplemental material.

The Journal of Cell Biology, Vol. 169, No. 1, April 11, 2005 151–165
http://www.jcb.org/cgi/doi/10.1083/jcb.200407058

neuronal growth cones polarize raft components during steering, and this polarization is essential for growth cone guidance (Guirland et al., 2004). Furthermore, two recent studies have provided evidence that sites of MT accumulation at the cell surface coincide with regions of the plasma membrane enriched in raft markers (Pardo and Nurse, 2003; Palazzo et al., 2004). It thus seems that cell surface sites enriched in rafts might coincide with sites where MTs interact with the cell membrane, but the mechanisms linking cell surface rafts to MT capture and organized motility at the cell surface are not clear.

Members of the Rho-type family of small GTPases, key molecular switches linking cell surface signaling to the regulation of actin dynamics, play major roles in regulating cell motility (Etienne-Manneville and Hall, 2002). In addition, Rho-type GTPases regulate processes that shape cell dynamics, such as the assembly and dynamics of focal contact sites (Small and Kaverina, 2003), and the dynamics of MTs (Rodriguez et al., 2003). Rho-type GTPases may thus promote the assembly of specific signaling complexes, possibly including $PI(4,5)P_2$-rich rafts, to link local signaling to actin-based motility and cell organization.

Here, we investigated whether and how $PI(4,5)P_2$-rich rafts accumulate and organize to influence protrusive motility at the cell surface. We show that signals triggering lamellipodial motility at the cell edge, induce a rapid local accumulation of dynamic cholesterol- and $PI(4,5)P_2$-rich raft-based plasmalemmal domains with unique turnover properties for acylated raft components and $PI(4,5)P_2$. We further show that the patches capture and stabilize MT plus ends through patch-associated IQGAP1. MTs in turn promote the clustering of raft patches into spatially focused and temporally stable domains, restraining and polarizing motility. Together, our results suggest a two-step model for local control of motility and polarization in which: (1) local signaling at the cell surface induces raft patching through $PI(4,5)P_2$ and Cdc42 to promote motility; and (2) clustering of the patches into more stable platforms through MTs and PKA polarizes and organizes motility. As there are extensive similarities among the molecular requirements for processes involving sustained polarized signaling at the cell surface, these principles for local control of signaling and polarization through raft assembly and organization likely apply to further cellular processes.

Results

$PI(4,5)P_2$-rich raft patches reflect distinct diffusion domains at the cell surface

To investigate how lipid rafts relate to protrusive motility at the cell surface, we stained quiescent, replated or PDGF-treated cells for the raft-associated components cholesterol (filipin), GAP43, and $PI(4,5)P_2$. Although quiescent cells did not exhibit obvious sites of cell surface raft concentrations, raft components in replated cells were concentrated in patches at cell surface ruffling lamellae, where they codistributed with intense labeling for f-actin (Fig. S1, available at http://www.jcb.org/cgi/content/full/jcb.200407058/DC1). Significantly, while cells attached and spread to a comparable extent in the absence or presence of cyclodextrin, raft disruption led to a near to complete loss of lamellipods, and a dramatic reduction of ruffling motility (Fig. S1; Grimmer et al., 2002).

To investigate the properties of raft accumulation sites associated with protrusive motility, we analyzed cells transfected with GFP (or RFP; tetrameric dsRed) fusion proteins targeting to lipid rafts. For the purpose of this study, PC12 cells cultured on a collagen substrate provided a particularly favorable experimental system, due to the comparatively large size of their raft patches. We found that a PLCδ1-PH-GFP construct (PHδ1-GFP) specifically targeting to plasmalemmal $PI(4,5)P_2$ (Tall et al., 2000), and an RFP construct targeted to the cytosolic face of cell surface rafts through a double-palmitoylated RFP construct (ppRFP) colocalized at prominent patches near the cell edge of living PC12 cells (Fig. 1 A). In contrast, when surface and intracellular membranes in the same living PC12 cells were labeled with the lipophilic dye DiD, which distributes homogeneously throughout the lipid phase of cellular membranes, no accentuation of the DiD signal was detected at cell surface sites highlighted by the raft markers (Fig. 1 A). Furthermore, live imaging with PHδ1-GFP, followed by fixation, permeabilization with saponin, and staining for raft markers yielded closely comparable labeling patterns before and after fixation (Fig. 1 B). We concluded that the patches reflect sites of $PI(4,5)P_2$ and raft marker accumulation at the surface of living cells.

The association of cell surface proteins and lipids with lipid microdomains does not by itself affect their diffusion rates in the membrane as determined in FRAP experiments (Kenworthy et al., 2004). To determine whether $PI(4,5)P_2$-rich raft patches might reflect plasmalemmal domains distinct from surrounding membranes at the cell surface, we performed a FRAP analysis in PC12 cells expressing double-palmitoylated GFP targeting to rafts (ppGFP). FRAP of ppGFP at homogeneously labeled ventral plasma membrane facing the substrate yielded rapid recovery rates comparable to published values, and edge-to-center gradients of fluorescence recovery consistent with lateral diffusion (Fig. 1 C). Similar rapid recovery rates were detected for dorsal surfaces outside patch areas (not depicted). In marked contrast, FRAP at dorsal (brightly labeled) patches was consistently slower (about threefold), and recovery patterns exhibited no evidence for edge-to-center gradients (Fig. 1 C). Similar slow FRAP values were obtained for raft-accumulating substrate facing podosomes, i.e., well-defined structures at the plasma membrane (Fig. 1 C). We concluded that $PI(4,5)P_2$-rich raft patches associated with protrusive motility reflect membrane compartments with distinct dynamic properties at the cell surface.

A rapid local accumulation of $PI(4,5)P_2$-rich raft patches at the cell edge anticipates protrusive motility

To investigate how the redistribution of cell surface raft patches relates to protrusive motility, we analyzed the short-term responses of PC12 cells to NGF. In the absence of NGF, PC12 cells exhibited a near to complete absence of protru-

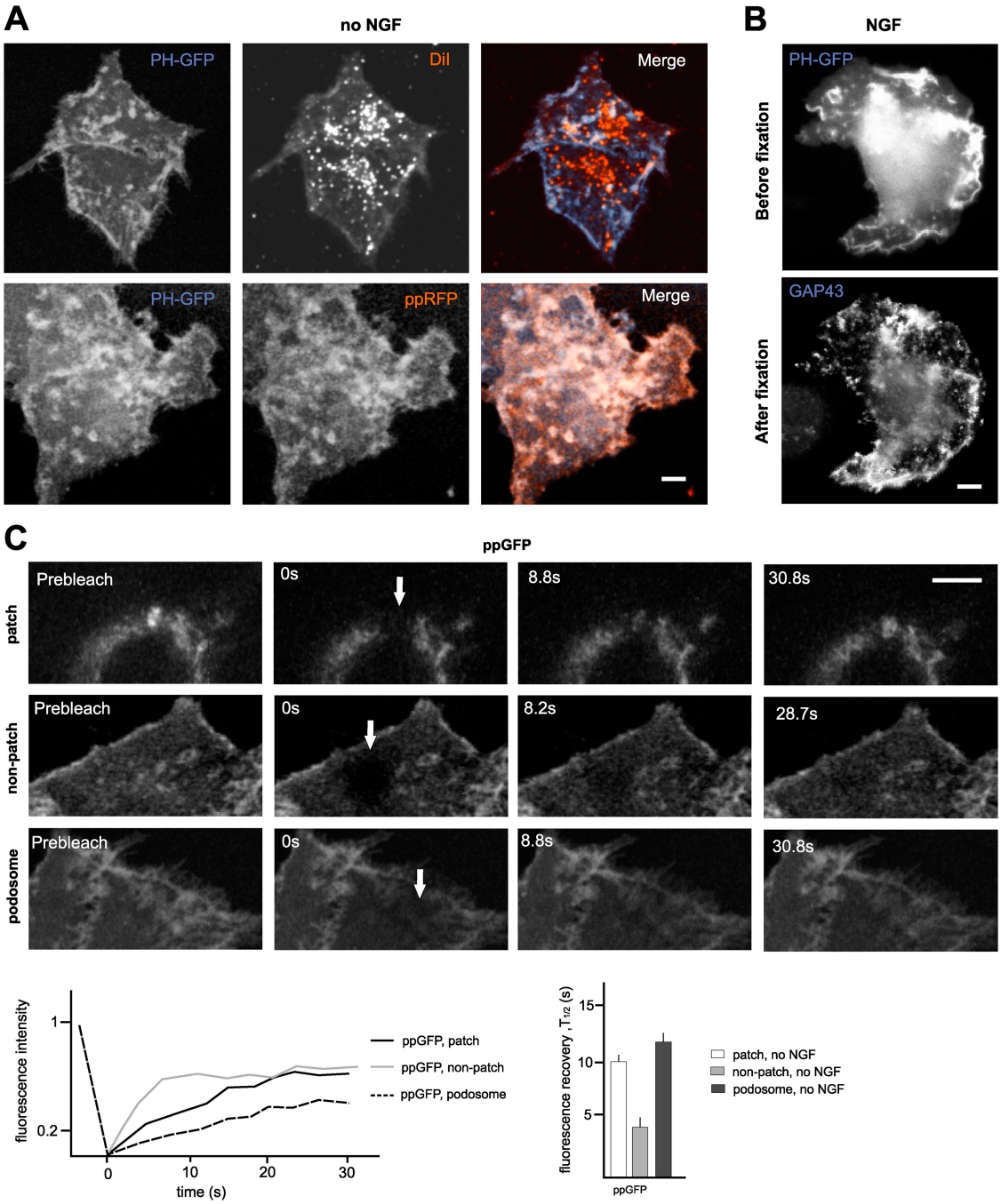

Figure 1. **Visualization and FRAP-based validation of PI(4,5)P_2-rich raft assemblies in living PC12 cells.** (A) Visualization of PI(4,5)P_2-rich raft assemblies in living cells. (Top) PHδ1-GFP highlights PI(4,5)P_2-rich patches that are not emphasized by the lipophilic dye DiD. (Bottom) Co-distribution of PI(4,5)P_2-rich raft patches visualized with PHδ1-GFP and ppRFP. The images are z-stacks including all planes of these double-labeled living cells. (B) Comparable labeling patterns for PI(4,5)P_2-rich raft complexes in living and fixed PC12 cells. The live-cell image (PH-GFP) was acquired 5′ after the addition of NGF. Fixative was added within 15–20 s after image acquisition, fixed cells were labeled for GAP43, and the PH-GFP-positive cell was retraced. (C) FRAP for ppGFP reveals specific immobilization of raft markers at PI(4,5)P_2-rich raft patches. PC12 cells in the absence of NGF. Images are single confocal sections (patch, confocal plane slightly above substrate; nonpatch and podosome, bottom plane of cells). Arrows indicate bleached area at end of photobleaching time. Representative FRAP curves (individual experiments) and average FRAP half-lives (n = 15) are also shown in the figure. Bars, 3 μm.

sive motility at the cell edge (Video 1, available at http://www.jcb.org/cgi/content/full/jcb.200407058/DC1). Upon the addition of NGF, phase-contrast time-lapse recordings revealed substantial protrusive motility, which started 45–60 s upon the addition of the growth factor, peaked at 4–8 min, and subsided after 15–20 min in the presence of NGF (Fig. 2 A; Video 2, available at http://www.jcb.org/cgi/content/full/jcb.200407058/DC1). Pretreatment of the cultures with 5 mM cyclodextrin, suppressed most NGF-induced protrusive motility, except for a brief phase of thin lamellae and spike extension at the cell edge (Fig. 2 A; Video 3, available at http://www.jcb.org/cgi/content/full/jcb.200407058/DC1).

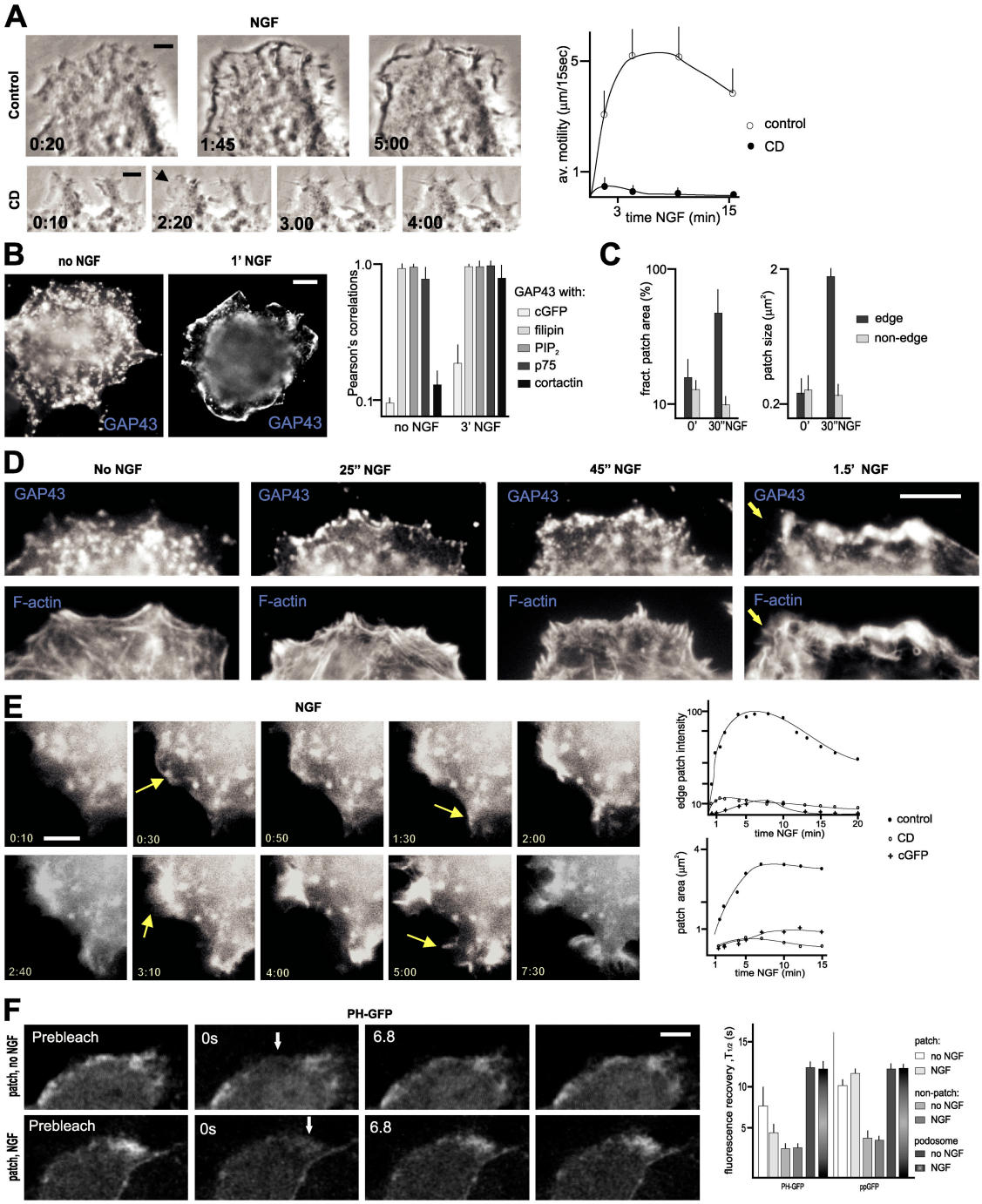

Figure 2. **Rapid redistribution and accumulation of PI(4,5)P_2-rich raft patches at the cell edge upon induction of protrusive motility.** (A) NGF-induced protrusive motility at the cell edge depends on raft integrity. (Left) Phase-contrast time-lapse recordings of PC12 cells treated with NGF in the absence or presence of (CD). Arrow indicates growth of a thin lamellipod in the presence of cyclodextrin (CD). (Right) Quantitative analysis of NGF-induced protrusive motility (forward and backward displacements of cell edge per unit time), without (control) and with cyclodextrin. $n = 15$ cells. (B) NGF induces a rapid redistribution of cell surface raft patches. (Left) redistribution of raft patches (GAP43) from the dorsal surface (no NGF) to the edge (1 min NGF) of NGF-treated cells. (Right) Co-distribution of raft-associated components at cell surface patches in PC12 cells in the absence and presence of NGF. Pearson's values of 1.0 reflect a complete overlap of compared signals. (C) Rapid redistribution of raft patches in NGF-treated cells. Fractional patch area: fraction of surface area labeled with raft marker (GAP43). Times: no NGF, 30'' NGF. $n = 15$. (D) Redistribution and accumulation of raft patches at the cell edge in response to NGF precedes actin rearrangements associated with lamellar and lamellipod motility. (E) Dynamics of NGF-induced cell surface PI(4,5)P_2 patches visualized with PHδ1-GFP. (Left) Live imaging of PH-GFP. Arrows at 0:30 and 1:30 indicate new cell edge PI(4,5)P_2-rich patches predicting lamellipodial motility; at 3:10, PI(4,5)P_2-rich domain extending with a lamellipod; at 5:00, appearance of a new distal domain. (Right) Quantitative analysis of cell edge PH-GFP patches in NGF-treated PC12 cells. Average values; control: $n = 15$; cyclodextrin and cGFP: $n = 4$. (F) Rapid, NGF-stimulated turnover of PI(4,5)P_2 at raft patches. Representative examples (left, panels on the right: 17.0 s) and quantitative analysis of FRAP half-lives (right) for PHδ1-GFP and ppGFP at and outside PI(4,5)P_2-rich raft patches. Images are single confocal sections. $n = 15$. Bars: (A–E) 3 μm; (F) 2 μm.

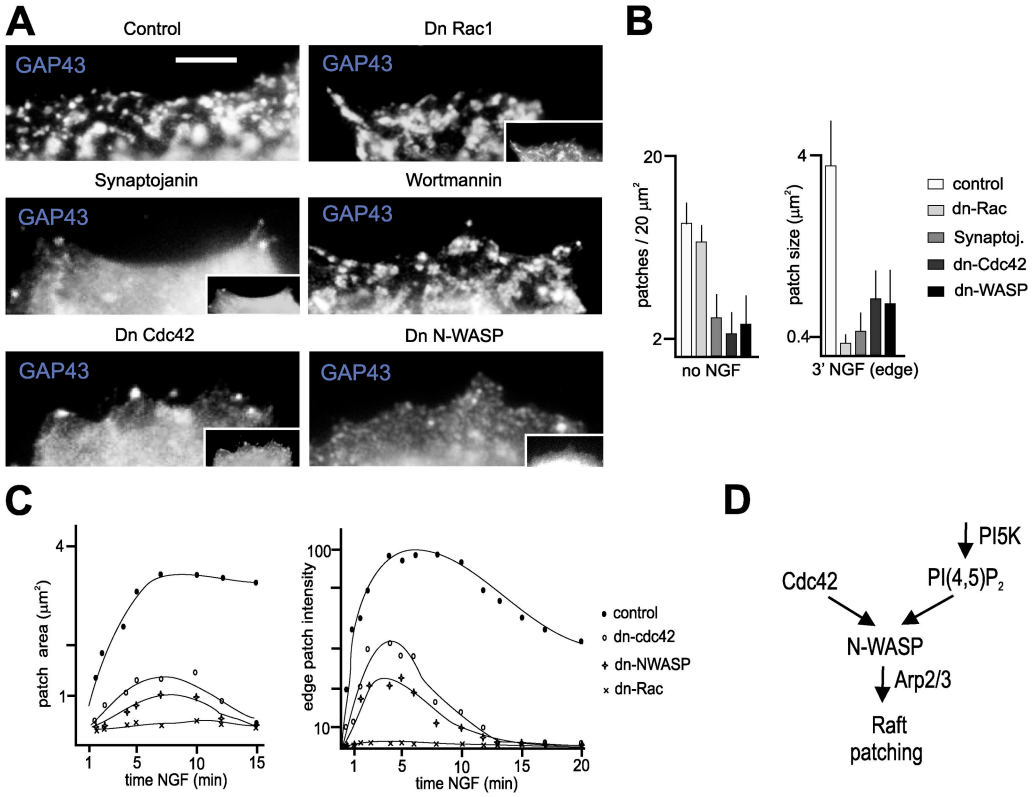

Figure 3. **Raft patch accumulation at the cell surface depends on PI(4,5)P_2, Cdc42, and N-WASP.** (A) Requirement for PI(4,5)P_2, Cdc42, and N-WASP to accumulate raft patches at the surface of naive PC12 cells (no NGF). (B) Quantitative analysis of experiments as shown in panel a. Raft marker: GAP43. n = 30 cells. (C) Impaired assembly and persistence of NGF-induced cell surface PI(4,5)P_2-rich patches in the presence of dn-Cdc42 or dn-N-WASP. Analysis of PH-GFP lives imaging recordings. Dn-Cdc42, dn-N-WASP: n = 10; dn-Rac: n = 4. (D) Proposed mechanism to induce cell surface raft patching. PI5K: PI-5-kinase. Bar, 2 μm.

Consistent with a critical role of rafts in promoting ruffling motility, NGF induced a rapid redistribution and gradual accumulation of PI(4,5)P_2-rich raft patches along the edge of PC12 cells (Fig. 2, B–D). The appearance of numerous, initially small raft patches at the cell edge was detectable from 20 s on, and preceded NGF-induced loss of stress fibers and focal adhesions (i.e., a process preceding protrusive motility; Fig. 2 D). Further raft patch accumulation accompanied the appearance (from 45–60 s on) of intensely labeled f-actin structures (Fig. 2 D) rich in Dynamin2, cortactin, and Arp3 at these same sites (i.e., a process coinciding with ruffling motility; see Fig. 4 B).

In the absence of NGF, cell surface PI(4,5)P_2-rich patches exhibited little dynamics and/or motility (PHδ1-GFP; unpublished data). Within 20–40 s upon the addition of NGF, new distinct PI(4,5)P_2-rich patches appeared on the surface of PC12 cells adjacent to the cell edge (Fig. 2 E; Videos 4 and 5, available at http://www.jcb.org/cgi/content/full/jcb.200407058/DC1). Individual patches behaved as coherent and highly dynamic surfaces for periods of up to 5 min and more (Fig. 2 E), and their positions correlated with those of protruding motility (>90% of new patch sites exhibited lamellipodial motility within the next 3 min). Although the patterns of PHδ1-GFP patch motility did in part overlap with ruffling lamellipods, they did not directly reflect the distribution of motile lamellae. Thus, thin substrate-associated protruding lamellae usually exhibited inverted (lowest at front) gradients of PHδ1-GFP signal, and raft marker signals were consistently low at the leading edge of thin protruding lamellae. We concluded that lamellipodial motility is preceded by a redistribution of cell surface rafts, and coincides with the accumulation of distinct PI(4,5)P_2-rich raft patch assemblies at sites exhibiting motility.

NGF enhances PI(4,5)P_2 turnover and reduces raft component exchange rates at cell surface raft patches

To explore the possibility that NGF might influence actin-based motility through the accumulation of PI(4,5)P_2 at leading edge raft patches, we performed FRAP experiments in cells expressing PHδ1-GFP, in the absence and presence of NGF. In the absence of NGF, FRAP values for PI(4,5)P_2 at patch, non-patch, and podosome regions of the plasma membrane resembled those for the raft marker ppGFP (Fig. 2 F). In contrast, NGF substantially accelerated PI(4,5)P_2 FRAP rates at raft patches, whereas it slightly slowed down corresponding FRAP values for ppGFP (Fig. 2 F). Neither ppGFP nor PHδ1-GFP FRAP rates outside raft patches or at podosomes were affected by NGF (Fig. 2 F). The differences in PHδ1-GFP recovery rates at and outside patches, as well as inside patches in the absence or presence of NGF argued against the possibility that exchange rates with unbound cytosolic pools of PHδ1-GFP were the rate limiting factor in these experiments. Instead, our findings suggest that PI(4,5)P_2 levels at raft patches are pri-

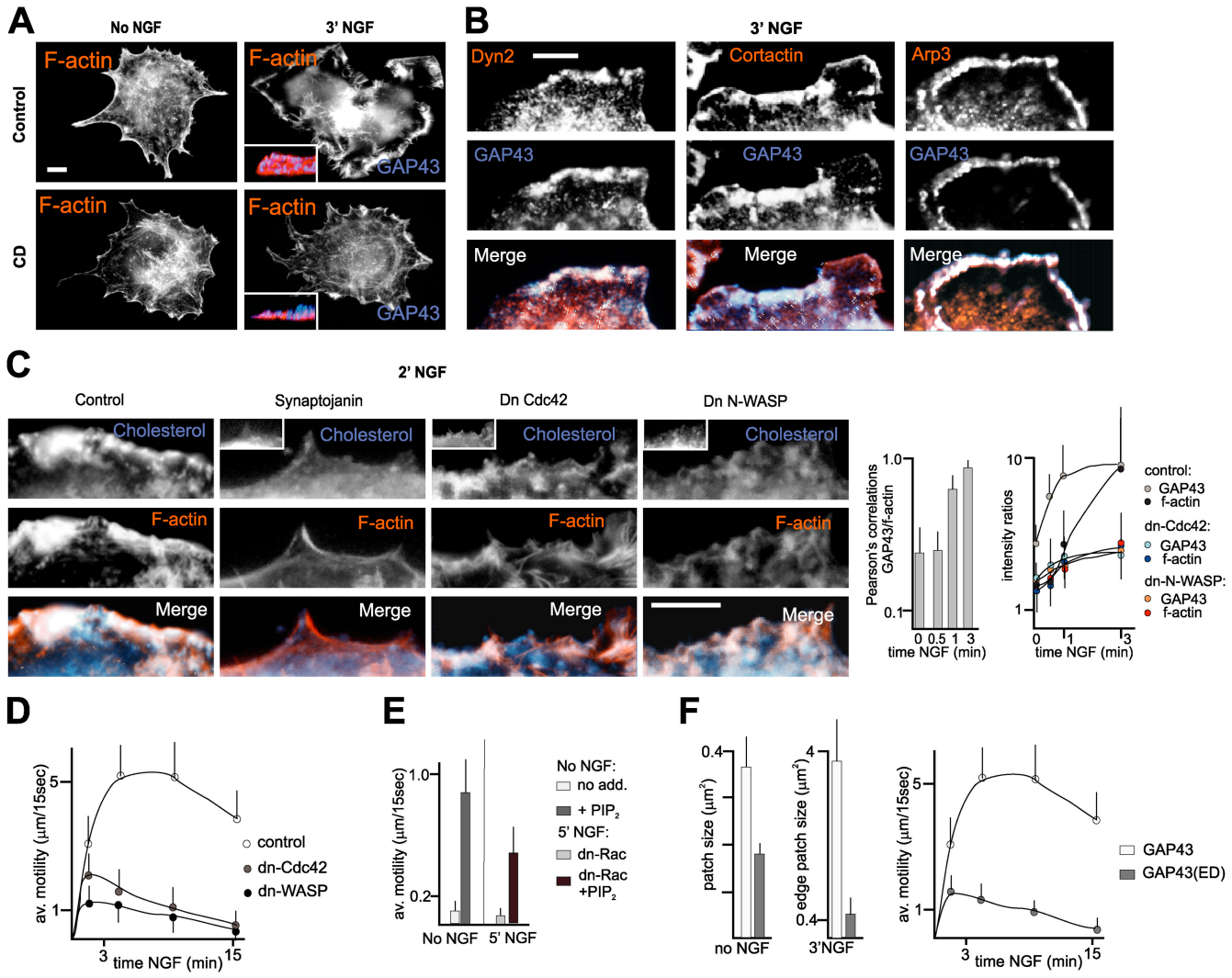

Figure 4. **Requirement for PI(4,5)P_2-rich raft patches to promote actin cytoskeleton accumulation and sustained protrusive motility at the leading edge.** (A) NGF-induced assembly of f-actin–rich lamellipods depends on raft integrity. The insets show representative x-z profiles of leading edges double labeled for GAP43 (blue, cell surface) and f-actin (orange). (B) Accumulation of proteins involved in actin-based membrane motility (Dynamin2, cortactin, and Arp3) at raft patches in NGF-treated PC12 cells. (C) Actin cytoskeleton accumulation at raft patches in NGF-treated cells. (Left) Prominent accumulation of f-actin at cell edge raft patches 2 min after the addition of NGF. (Right) Co-distribution of raft marker and f-actin signal, and relative raft and f-actin labeling intensities at cell edge patches. $n = 10$ cells. (D) Reduction in the extent and persistence of NGF-induced protrusive motility in cells expressing dn-Cdc42 or dn-N-WASP. Analysis of phase-contrast time-lapse recordings. Average values; $n = 10$ cells. (E) Exogenously added PI(4,5)P_2 promotes lamellipod motility in the absence of NGF, and some NGF-induced motility in the presence of dn-Rac. $n = 8$ cells. (F) PC12 cells stably expressing a GAP43(ΔED) construct interfering with the accumulation of raft patches at the cell surface exhibit reduced NGF-induced lamellipodial motility. Raft patches: $n = 30$ cells; motility: $n = 10$ cells. Bars, 3 μm.

marily controlled through hydrolysis and synthesis rates of PI(4,5)P_2 at the patches, which are accelerated by NGF.

Cell surface raft patching depends on PI(4,5)P_2, Cdc42, and N-WASP

We next addressed the mechanisms underlying the accumulation of PI(4,5)P_2-rich raft patches associated with cell surface motility. To discriminate between mechanisms inducing motility itself, and specific requirements to induce raft patching, we initially analyzed PC12 cells cultured in the absence of NGF, which exhibited well-defined raft patches on their dorsal surface. We found that overexpression of the PI(4,5)P_2 phosphatase synaptojanin (Cremona and De Camilli, 2001) or of dominant-negative (dn) Cdc42 abolished raft patching in quiescent cells, whereas dn-Rac and the PI3-kinase inhibitor Wortmannin (and dn-Rho; not depicted) did not (Fig. 3, A and B). Furthermore, a dn-N-WASP construct (Lommel et al., 2001) effectively suppressed cell surface raft patches in PC12 cells (Fig. 3, A and B), and so did disruption of the actin cytoskeleton with cytochalasin (not depicted).

Dn-Cdc42 or dn-N-WASP did not prevent the initial accumulation of PI(4,5)P_2 at the edge of NGF-treated cells, but PI(4,5)P_2-rich patches were abnormally small, weakly labeled, and short lived (Fig. 3, B and C; Video 6, available at http://www.jcb.org/cgi/content/full/jcb.200407058/DC1). In contrast, dn-Rac suppressed the appearance of new PI(4,5)P_2 signal, raft patches, and motility in NGF-treated cells (Fig. 3, B and C). A specific inhibitor of PI(4,5)P_2-hydrolyzing PLC en-

zymes (U73122) failed to restore any $PI(4,5)P_2$ accumulation in the presence of dn-Rac, and inhibiting PI3-kinase did not suppress NGF-induced $PI(4,5)P_2$ accumulation and patching in the absence of dn-Rac (not depicted), suggesting that it might be the failure to locally generate $PI(4,5)P_2$ in response to NGF that prevented raft patching in the presence of dn-Rac. In support of this interpretation, carrier-mediated delivery of $PI(4,5)P_2$ partially rescued NGF-induced raft patch accumulation in the presence of dn-Rac (not depicted; see Fig. 4 E), and overexpressing synaptojanin suppressed NGF-induced actin remodeling and lamellipod formation in PC12 cells (not depicted). We concluded that the sustained accumulation of $PI(4,5)P_2$-rich rafts into distinct patches depends on a specific mechanism involving $PI(4,5)P_2$, Cdc42, N-WASP, and actin cytoskeleton integrity (Fig. 3 D).

Raft patch accumulation is required to promote sustained protrusive motility at the leading edge

We next investigated how the accumulation of $PI(4,5)P_2$-rich rafts into patches might influence cell surface motility. As expected, NGF induced a redistribution of the actin cytoskeleton in PC12 cells, from a stress fiber pattern characteristic of quiescent cells to a prominent ruffling lamellipodial pattern, and this process depended on raft integrity (Fig. 4 A). Furthermore, we detected a pronounced accumulation of Dynamin2, cortactin, Arp3 and f-actin at raft patches along the cell edge in the presence of NGF (Fig. 4, B and C). This accumulation was greatly reduced in cells overexpressing dn-Cdc42 or dn-N-WASP, and abolished in cells overexpressing Synaptojanin (Fig. 4 C). Accordingly, phase-contrast time-lapse recordings revealed that in the presence of dn-Cdc42 or dn-N-WASP, both intensity and duration of NGF-induced cell surface motility were greatly reduced (Fig. 4 D). Furthermore, carrier-mediated delivery of $PI(4,5)P_2$ induced spontaneous cell edge motility in the absence of NGF, and rescued some NGF-induced motility in the presence of dn-Rac (Fig. 4 E). Together (see also Online supplemental material describing data of Fig. 4 F), these results suggest that the local accumulation of raft patches in a process requiring $PI(4,5)P_2$, Cdc42, and N-WASP enhances and sustains signaling for actin assembly and protrusive motility in NGF-treated cells.

Capture and stabilization of MTs at cell edge raft patches through IQGAP1

Although patch accumulation was required to promote sustained protrusive motility, and although sites where raft patches accumulated were predictive of where motility would develop along the cell edge, their actual positions did not directly coincide with those of motile lamellipods. This raised the issue of how patch and lamellipod distributions might be related causally. To explore the possibility that this relation might involve

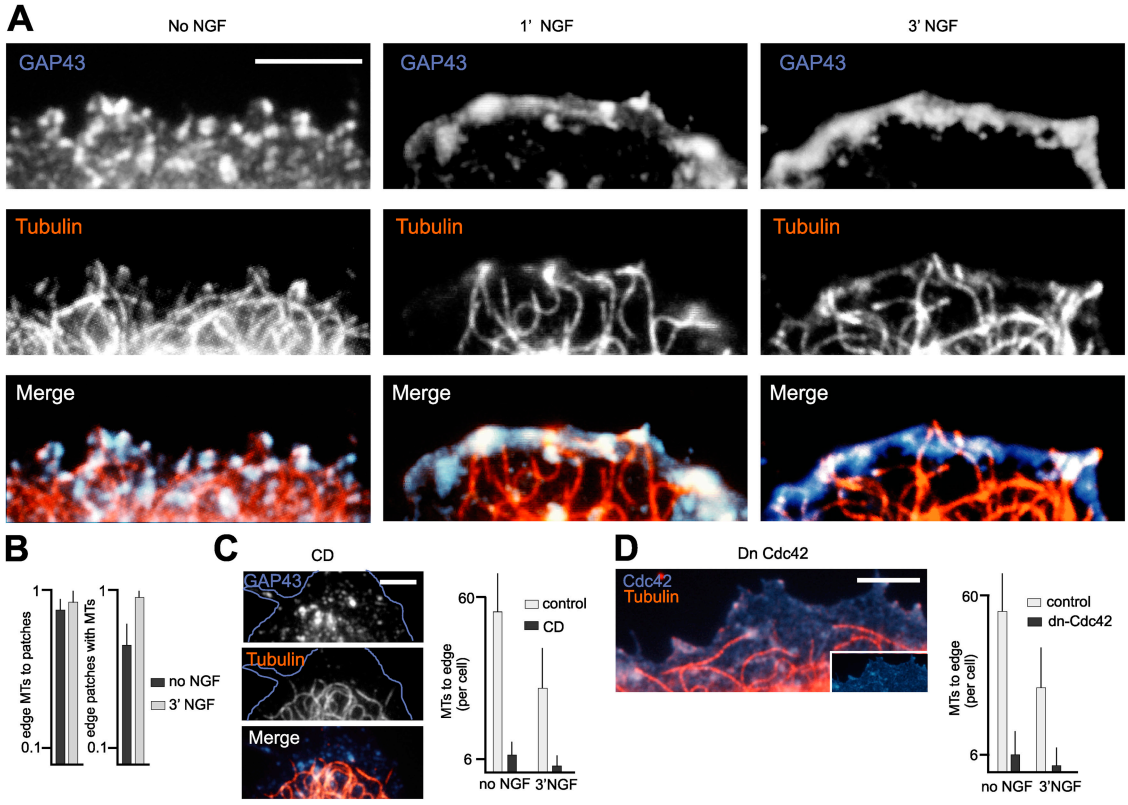

Figure 5. **Capture of MTs at cell edge raft patches.** (A) MT ends associate with cell edge raft patches in naive and NGF-treated PC12 cells. (B) Quantitative analysis of data as shown in A. The extents to which MTs specifically associate with raft patches at the cell edge are given in fractional values (value of 1 = 100%). $n = 30$ cells. (C) MT capture at the cell edge depends on raft integrity. Raft disruption (CD, 10′) leads to loss of MTs associated with the cell edge. (D) MT capture at the cell edge depends on raft patching. $n = 30$ cells. Bars, 2 μm.

MTs, we compared the distributions of raft patches and MTs near the cell edge. We found a striking codistribution of MT ends with raft patches at the edge of quiescent and NGF-treated PC12 cells (Fig. 5, A and B), where MTs were stabilized (Fig. S2, available at http://www.jcb.org/cgi/content/full/jcb.200407058/DC1). Disruption of lipid rafts with cyclodextrin led to a near to complete loss of MTs targeting the cell edge (Fig. 5 C), and overexpression of dn-Cdc42 (or dn-N-WASP; not depicted), greatly reduced MT capture at the edge of these cells (Fig. 5 D), suggesting that capture specifically depended on the presence of raft patches.

To investigate the mechanism through which MTs are captured at raft patches we analyzed the distribution of proteins implicated in MT capture or targeting at the cell edge. We found that the MT-plus-end–associated protein APC, which has been implicated in targeting of MTs to leading edges (Näthke et al., 1996), also codistributed with cell edge raft patches (Fig. S3, available at http://www.jcb.org/cgi/content/full/jcb.200407058/DC1). However, this association depended on both, raft and MT integrity, suggesting that APC is brought to the patches by MTs. We further found that IQGAP1 accumulated at the cell edge, where it codistributed with raft patches (Fig. 6 A). Although the association of IQGAP1 with the cell edge depended on raft integrity, it was only partially affected by a disruption of MTs with nocodazole (Fig. 6 A). To investigate whether the presence of IQGAP1 is required for MTs to be captured at cell edge patches, we performed knockdown (RNAi) experiments for IQGAP1. We found that while mock-transfected cells continued to capture MTs at leading edge raft patches, down-regulation of IQGAP1 led to a near to complete loss of MTs targeting the leading edge in these cells (Fig. 6,

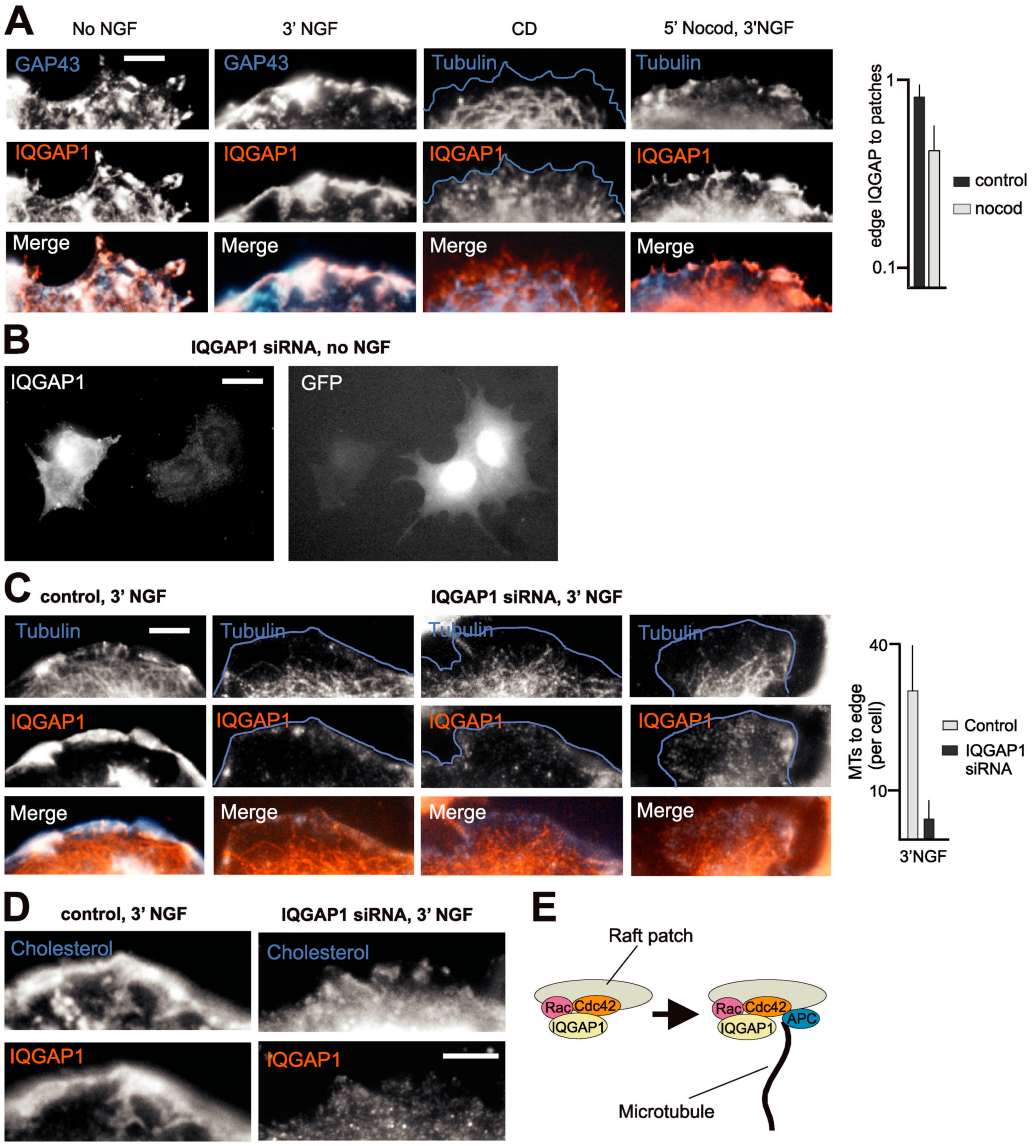

Figure 6. **Raft patches capture MTs through IQGAP1.** (A) Association of IQGAP1 with cell edge raft patches. The accumulation of IQGAP1 at the cell edge depended on raft integrity, but not on MT integrity. Blue outline (CD), cell edge. Quantitative analysis (fractional values): no NGF, $n = 30$ cells. (B) Knockdown of IQGAP1 in PC12 cells. Transfected cells coexpressed GFP. (C) Capture of MTs at raft patches depends on IQGAP1. Quantitative analysis of MTs to edge: $n = 30$ cells. (D) Fragmentation of raft patches (cholesterol) in the absence of IQGAP1. (E) Model of how IQGAP1 may provide a physical link, from cell edge raft patches (Rac-GTP and Cdc42-GTP) to MT plus-ends. Bars: (A, C, and D) 2 μm; (B) 5 μm.

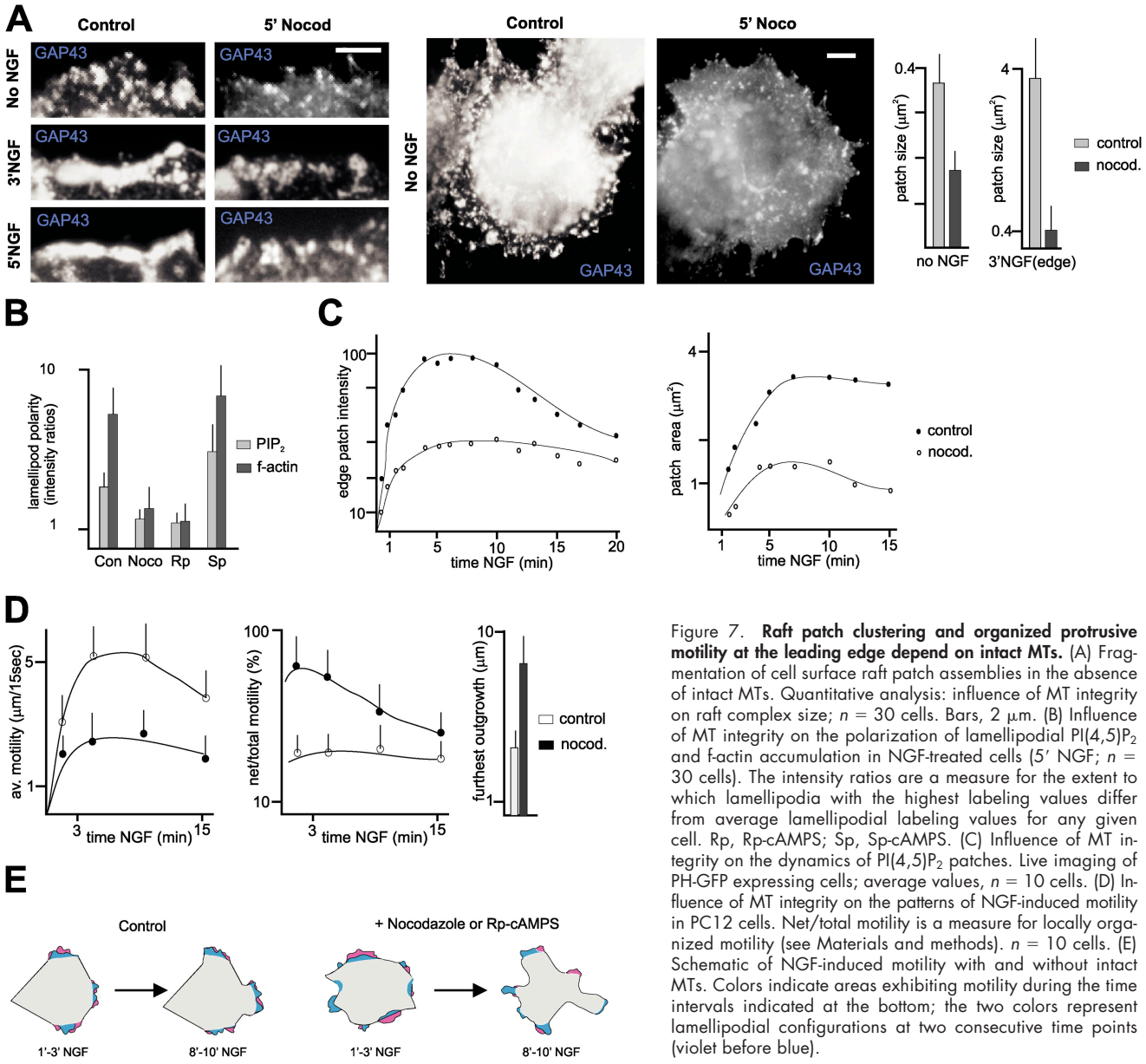

Figure 7. **Raft patch clustering and organized protrusive motility at the leading edge depend on intact MTs.** (A) Fragmentation of cell surface raft patch assemblies in the absence of intact MTs. Quantitative analysis: influence of MT integrity on raft complex size; $n = 30$ cells. Bars, 2 μm. (B) Influence of MT integrity on the polarization of lamellipodial PI(4,5)P_2 and f-actin accumulation in NGF-treated cells (5′ NGF; $n = 30$ cells). The intensity ratios are a measure for the extent to which lamellipodia with the highest labeling values differ from average lamellipodial labeling values for any given cell. Rp, Rp-cAMPS; Sp, Sp-cAMPS. (C) Influence of MT integrity on the dynamics of PI(4,5)P_2 patches. Live imaging of PH-GFP expressing cells; average values, $n = 10$ cells. (D) Influence of MT integrity on the patterns of NGF-induced motility in PC12 cells. Net/total motility is a measure for locally organized motility (see Materials and methods). $n = 10$ cells. (E) Schematic of NGF-induced motility with and without intact MTs. Colors indicate areas exhibiting motility during the time intervals indicated at the bottom; the two colors represent lamellipodial configurations at two consecutive time points (violet before blue).

B and C). In addition, leading edge raft patches in the absence of IQGAP1 were strikingly small, and were not concentrated into a few major patches in NGF-treated cells (Fig. 6 D). We concluded that cell edge raft patches capture MT plus ends through IQGAP1 (Fig. 6 E).

Raft patch clustering through MTs is required to organize protrusive motility at the cell surface

To investigate how MTs might influence cell surface raft patches and NGF-induced motility, we analyzed PC12 cells treated with nocodazole. Treatments sufficient to disrupt most MTs in PC12 cells (3 min nocodazole) led to a marked fragmentation of raft patches in the absence of NGF (Fig. 7 A). Furthermore, while some raft patches did accumulate at the cell edge in response to NGF, they failed to assemble in larger clusters and to coincide with intense phalloidin signals in the presence of nocodazole (Fig. 7, A and B). Analysis of PI(4,5)P_2-rich patch dynamics in living NGF-treated cells revealed two consistent alterations in the absence of intact MTs: (1) a major impairment in PI(4,5)P_2-rich patch condensation and persistence; and (2) rapid forward dissipation of PI(4,5)P_2-rich raft patches, coinciding with the emergence of rapidly advancing motile lamellae at the cell edge (Fig. 7 C; Video 7, available at http://www.jcb.org/cgi/content/full/jcb.200407058/DC1).

Phase-contrast time-lapse imaging revealed that NGF-treated cells with disrupted MTs consistently lacked coherent, spatially defined regions of sustained lamellipodial motility (i.e., regions exhibiting rapidly alternating forward and backward protrusive motility). This was reflected in the initial appearance of multiple small motile lamellae, followed by apparently unrestrained large-scale motility, leading to the formation of highly heterogeneous protrusions in these cells (Fig. 7, D and E; Video 8, available at http://www.jcb.org/cgi/content/

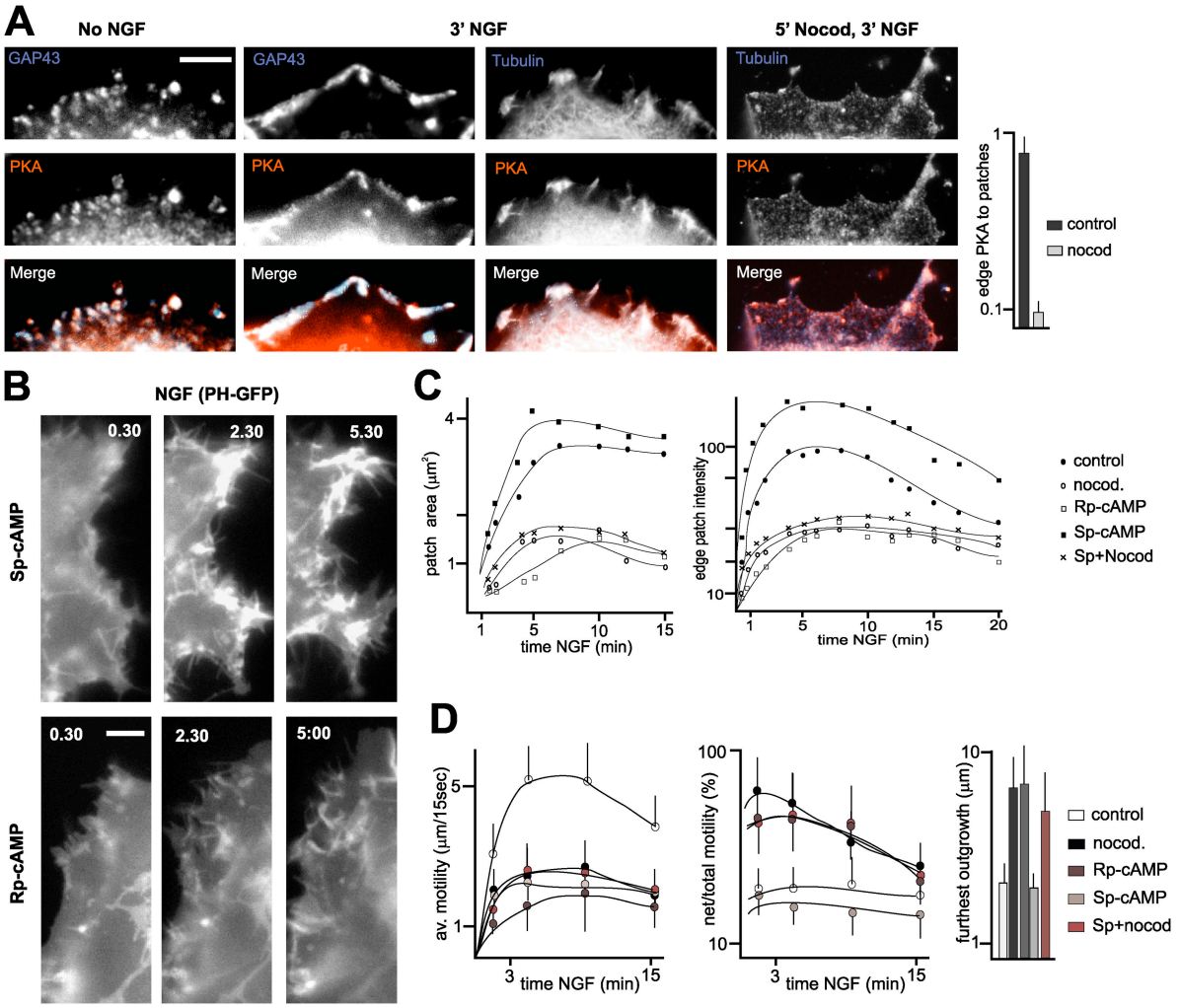

Figure 8. **MTs target PKA to cell edge raft patches, to promote patch clustering and spatially constrain protrusive motility.** (A) Targeting of PKA to cell edge raft patches through MTs. Quantitative analysis: no NGF, $n = 30$ cells. (B) The activity of PKA promotes PI(4,5)P_2 signal (PHδ1-GFP) accumulation and patch compaction at the cell edge. Bars, 2 μm. (C) Rp-cAMPS mimics the effects of nocodazole on PH-GFP patch dynamics, whereas Sp-cAMPS enhances patch clustering in a MT-dependent manner. Average values; $n = 10$ cells. (D) Rp-cAMPS mimics the effects of nocodazole on NGF-induced motility, and MT disruption suppresses any effect of Sp-cAMPS on leading edge motility. $n = 10$ cells.

full/jcb.200407058/DC1). Significantly, and in contrast to treatments interfering with raft patching, nocodazole did not affect the duration of NGF-induced motility, and only partially affected its intensity (Fig. 7 D). These observations provide evidence that MT integrity is specifically required to promote the local concentration of PI(4,5)P_2-rich patches into few stable clusters, and to promote spatially focused and temporally stable ruffling motility at the cell edge.

MTs target PKA to cell edge raft patches, to promote clustering and organize motility in response to cAMP

In a search for mechanisms that might mediate the effects of MTs on leading edge raft clustering and the organization of cell surface motility, we focused on PKA, a protein kinase that has been implicated in regulating motility at the leading edge (O'Connor and Mercurio, 2001). We found that the regulatory subunit of PKA (RII) accumulated at leading edge PI(4,5)P_2-rich raft patches, where it codistributed with MTs (Fig. 8 A). Disruption of cell surface rafts with cyclodextrin induced a loss of RII from the cell edge (not depicted). In addition, disruption of MTs led to a near to complete loss of RII from cell edge raft patches (Fig. 8 A), suggesting that RII is delivered to these patches through MTs.

To investigate a possible involvement of PKA-mediated signaling in the local regulation of raft patch clustering and cell surface protrusive motility by MTs, we used a membrane-permeable agonist of cAMP (Sp-cAMPS), or a membrane-permeable antagonist of cAMP (Rp-cAMPS) of PKA. Sp-cAMPS accelerated the appearance of PI(4,5)P_2 clusters at the cell edge in response to NGF, enhanced their compaction, and prolonged their half-lives (Fig. 8, B and C). This was reflected in a sustained focusing and restriction of small-scale protrusive motility to a few sites along the cell edge (Video 9, available at http://www.jcb.org/cgi/content/full/jcb.200407058/DC1; Fig. 8, B and D). In contrast, Rp-cAMPS interfered with raft clustering, and reduced patch PI(4,5)P_2 labeling intensity and actin accumulation at lamellipods (Fig. 8, B and C; Video 10, available at

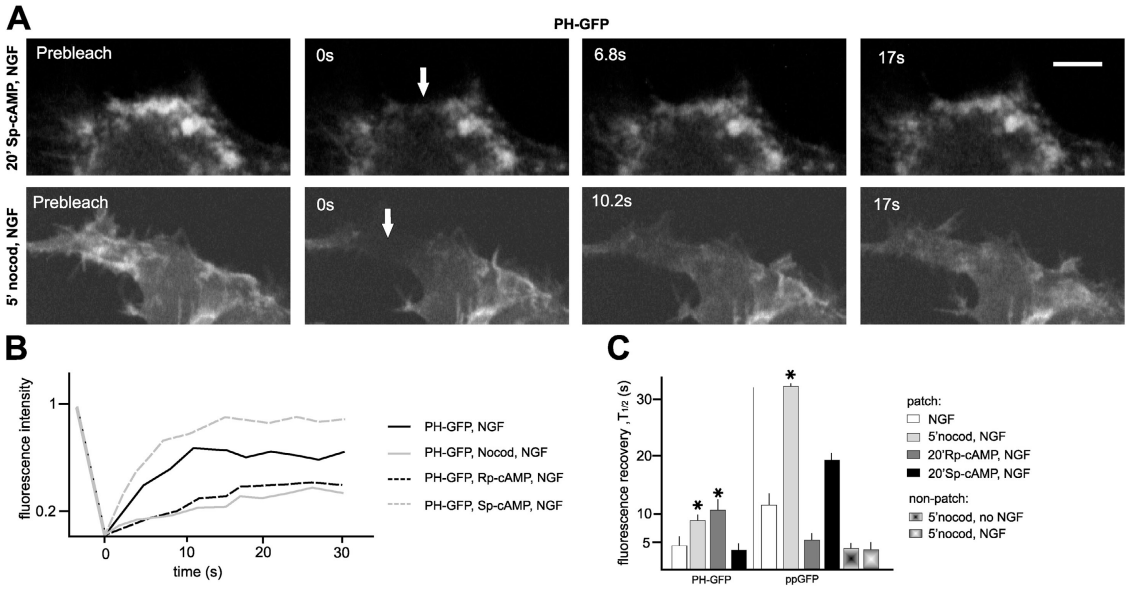

Figure 9. **MTs and cAMP augment FRAP rates for PI(4,5)P_2 at raft patches.** All experiments: PC12 cells treated with NGF. (A) Representative examples of PHδ1-GFP FRAP at patches in the presence of the cAMP analogue Sp-cAMPS or nocodazole. Single confocal sections; arrows point to bleached area at end of photobleaching time (0 s after photobleaching). Bar, 2 μm. (B) Representative FRAP curves (normalized) for PHδ1-GFP at raft patches. (C) Quantitative analysis of FRAP experiments for PHδ1-GFP and ppGFP at raft patches, with or without intact MTs, Sp-cAMPS or Rp-cAMPS. The values are FRAP half-lives; $n = 15$. Asterisks in these experiments indicate that fluorescence did not recover to original values (B, curves), and half-lives are given for plateau values.

http://www.jcb.org/cgi/content/full/jcb.200407058/DC1). This was reflected in a marked enhancement of unfocused and uncontained large-scale motility (Fig. 8 D). Although the effects of Rp-cAMPS were clearly reminiscent of those induced by nocodazole, the cAMP antagonist did not affect the capture of MTs at cell edge raft patches (not depicted). Consistent with the notion that Sp-cAMPS and Rp-cAMPS acted through PKA delivered to the leading edge by MTs, neither the agonist nor the antagonist affected raft assembly and leading edge motility in the presence of nocodazole (Fig. 8, C and D). We conclude that one mechanism through which MTs organize motility at the leading edge involves the local delivery of PKA at raft patches, to promote their clustering.

MTs and cAMP enhance the turnover of PI(4,5)P_2 and reduce that of a membrane-associated raft component at raft patches

To investigate the mechanisms through which MTs and cAMP influence PI(4,5)P_2-rich raft clustering, we performed FRAP experiments with PHδ1-GFP and ppGFP. Disruption of MTs led to a twofold reduction in the turnover rate of PI(4,5)P_2, and a more than threefold reduction in the turnover rate of ppGFP, specifically at patches (Fig. 9, A–C). Inhibition of PLC enzymes (U73122, 1 μm) did not noticeably enhance PI(4,5)P_2 levels at patches in the presence of nocodazole (not depicted), suggesting that the reduced PI(4,5)P_2 levels more likely reflect reduced local synthesis in the absence of intact MTs. As predicted, Rp-cAMPS mimicked the inhibitory effect of nocodazole on PI(4,5)P_2 FRAP, whereas Sp-cAMPS further accelerated the turnover rate of PI(4,5)P_2 at patches (Fig. 9, A–C). Significantly, Rp-cAMPS did not mimic the effect of nocodazole on ppGFP FRAP rates at patches (Fig. 9 C). Thus, whereas nocodazole greatly slowed down the turnover of ppGFP at patches, Rp-cAMPS accelerated it more than twofold (Fig. 9 C). This result suggests that the turnover of ppGFP at patches involves MT-dependent trafficking of vesicles, and that the exchange of ppGFP through trafficking is inversely correlated to the degree of clustering of the patches. In support of this interpretation, Sp-cAMPS, which enhanced PI(4,5)P_2 patch clustering, led to a reduction in the turnover rate of ppGFP at patches (Fig. 9 C). Together, these results suggest that MTs, PKA and ultimately cAMP levels, influence PI(4,5)P_2-rich patch clustering through their effects on patch PI(4,5)P_2 metabolism and levels, and that increases in patch clustering lead to corresponding reductions in the rates of raft trafficking to and from the clusters.

Discussion

We have investigated mechanisms of cell surface PI(4,5)P_2-rich raft accumulation associated with motility, and their role in regulating protrusive motility at the cell edge. We show that signals initiating protrusive lamellipodial activity trigger local raft patching processes depending on PI(4,5)P_2, Cdc42, and N-WASP, which lead to the accumulation of distinct plasmalemmal domains rich in PI(4,5)P_2 and raft markers. We further show that these domains capture and stabilize MT plus ends through patch-associated IQGAP1. MTs in turn promote the clustering of raft patches into spatially focused and temporally stable domains, restraining and polarizing motility. In the following sections we discuss properties of these novel mechanisms, their proposed roles in organizing motility, and how these findings provide a framework to integrate related observations on how cell surface dynamics interfaces with cell polarity and organization.

PI(4,5)P_2-rich raft patches: distinct plasmalemmal domains associated with protrusive motility

We have provided evidence for the local accumulation of distinct PI(4,5)P_2- and raft-rich assemblies (patches) specifically associated with lamellipodial protrusive motility at the cell surface. These results provide an experimental paradigm to investigate how lipid rafts can contribute to local control of signaling at the cell surface. Thus, whereas the existence of cholesterol- and sphingolipid-enriched lipid microdomains, and their importance in cell trafficking and motility are well established (Golub et al., 2004; Wilson et al., 2004), whether and in what ways lipid rafts can organize into higher order domains at defined sites on the cell surface had remained controversial. Our finding that FRAP values for ppGFP at patches were substantially slower than those detected outside the patches provides evidence that lateral diffusion into and out of the patches is restricted. That FRAP for ppGFP at patches was greatly reduced in the absence of intact MTs, suggests that it might involve directed vesicle trafficking to and from the patches. Accordingly, in addition to accumulating raft-associated components promoting actin dynamics and cell signaling, PI(4,5)P_2-rich raft patches may provide distinct domains for raft-dependent trafficking at the cell surface. Such domains may, for example, be involved in the recycling and resensitization of cell surface receptors promoting signaling for motility.

PI(4,5)P_2- and Cdc42-dependent raft patching promotes sustained protrusive motility

Our studies provide evidence that the accumulation of rafts in patches at the cell surface depends on signals by Cdc42, PI(4,5)P_2, and N-WASP. This signaling mechanism ties in well with recent studies addressing mechanisms of cell motility regulation. Thus, integrin-dependent raft recruitment (del Pozo et al., 2004) may operate upstream of raft patching, patching regulation could ensure tight spatial regulation of motility through Cdc42-recruiting complexes at the cell membrane, and tight dynamic regulation of motility through PI(4,5)P_2 synthesis and hydrolysis (Fig. 10 A). Anchorage of activated N-WASP to raft-associated components may direct specific patterns of Arp2/3-mediated actin polymerization, to assemble membrane-associated actin scaffolds restricting the diffusion of signaling components. Although our experiments do not address directly the mechanism through which N-WASP promotes raft patching, we speculate that this might involve spatial containment through actin filament bundles, and adaptor proteins such as LAT (in T cells) and GAP43-like proteins (Golub et al., 2004).

We find that raft patching is required to promote and sustain motility at the leading edge. This is consistent with reports that the disruption of rafts diminished responses such as membrane ruffling and pinocytosis, and prevented sustained activation of actin dynamics in neutrophils (Grimmer et al., 2002; Pierini et al., 2003). As PI(4,5)P_2-rich platforms assembled at regions of prospective motility, these results suggest that assembled rafts provide spatial domains of enhanced signaling for motility. The patches may also contribute to sustain signals for protrusive motility through recycling and trafficking of signaling components at patches (Huang et al., 2004). In addition, locally regulated dynamics of the patches might contribute to distinct forms of actin-based protrusive motility such as protrusive lamellae (Mouneimne et al., 2004) and ruffling lamellipods (Fig. 10 A).

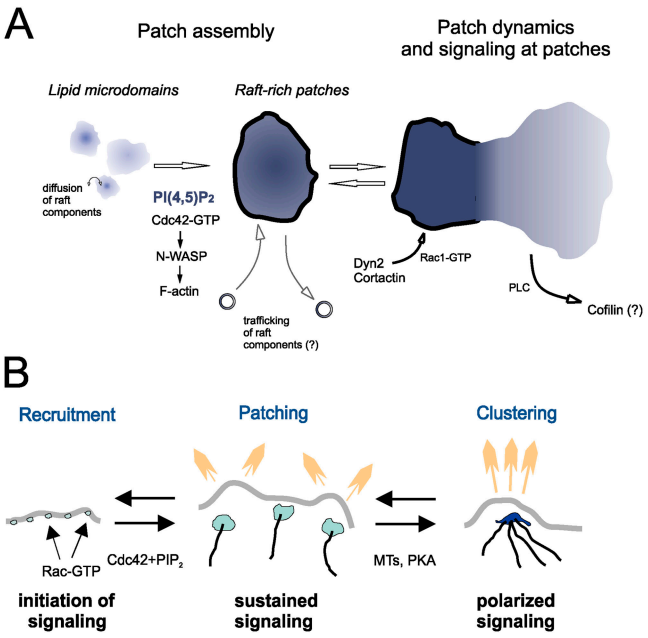

Figure 10. **Proposed role of PI(4,5)P_2-rich raft assemblies in regulating protrusive motility at the cell surface.** (A) Proposed model of how local PI(4,5)P_2 metabolism, together with Cdc42, drives the accumulation and dissipation of dynamic PI(4,5)P_2-dependent raft-rich patches, which provide signaling platforms for protrusive motility at the cell surface. (B) Proposed model of leading edge motility control through PI(4,5)P_2-rich raft assemblies and MTs. MTs captured at raft patches through IQGAP1 target PKA to the leading edge, promoting clustering of raft patches by enhancing PI(4,5)P_2 accumulation at patches. This leads to a focusing and polarization of signaling and motility.

Mechanism of MT-dependent clustering of PI(4,5)P_2-dependent raft patches

Our results provide evidence that there is a specific association between MT plus ends and plasmalemmal PI(4,5)P_2-dependent raft patches. In addition, we find a requirement for patch IQGAP1 in the capture of MTs at raft patches. IQGAP1 might specifically couple motility receptor activation and the recruitment of Rac-GTP and Cdc42-GTP to raft patches, to the capture of MTs at those raft patches (Fukata et al., 2002; Yamaoka-Tojo et al., 2004). The mechanisms through which MTs target to rafts at the cell edge could involve extension along actin filament bundles (Palazzo et al., 2004), and the selective regulation of MT dynamics near the cell edge (Rodriguez et al., 2003). The arrangement of MTs with respect to rafts would be consistent with a "pause" mode of interaction, in which MTs deliver components to defined sites at the cell edge, including PKA. Our results are reminiscent of findings that Cdc42 signaling defines sites of MT capture at the cell surface in yeast and in polarized astrocytes (Gundersen et al., 2004; Etienne-Manneville and Hall, 2003), and it will be interesting

to determine whether cell surface raft assemblies are also involved in those experimental settings.

We show that the mechanisms through which MTs promote patch clustering at the leading edge include delivery of PKA, whose activity promoted clustering and focused motility. This provides a potential mechanism to couple local signaling to adenylate cyclases and phosphodiesterases to the organization and steering of motility at the leading edge. We further show that MTs and cAMP enhance the accumulation and turnover rates of $PI(4,5)P_2$ at patches, a process well correlated with the extent of patch clustering. Patch clustering through MTs and cAMP may thus involve enhanced $PI(4,5)P_2$ accumulation, to augment the anchorage of raft patches to the cortical cytoskeleton, reducing their lateral spread and dynamics (Raucher et al., 2000). Because PKA can activate Rac and inhibit Rho, we speculate that one possible mechanism may involve the activation of PI5-kinase downstream of MTs, PKA, and Rac. Such a mechanism would be consistent with the observation that overexpressing PI5-kinase led to a dramatic condensation of cell edge raft patches and a reduction of NGF-induced motility in these cells (unpublished data).

Organization of protrusive motility by MTs through clustering of raft patches

This study provides novel evidence about the role of MTs in cell surface motility. Our results are in good agreement with previous reports that MT integrity is needed to contain and steer motility (Gordon-Weeks, 2004; Guirland et al., 2004), and provide a candidate mechanism involving the clustering and spatial confinement of raft patches that promote motility. Together, our results suggest a model whereby moderate cell surface local $PI(4,5)P_2$ levels, together with Cdc42, drive the assembly of $PI(4,5)P_2$-dependent raft-based plasmalemmal domains promoting motility, whereas higher $PI(4,5)P_2$ levels at these domains, induced through MTs and PKA, reversibly enhance their compaction and anchorage to the cell cortex, restraining motility (Fig. 10 B). This tight spatial and temporal regulation of motility through cell surface $PI(4,5)P_2$-rich raft patches and MTs could provide an exquisitely sensitive mechanism for directed cell migration and neuronal growth cone navigation. There are striking similarities between processes of cell surface domain patching and polarized clustering in cell motility, cytokinesis, and synapse formation. These include the spatio-temporal sequences of signaling platform assembly, and their molecular requirements (Weston et al., 2000; Wu et al., 2003). The mechanisms of raft-based patching and clustering reported in this study may therefore reflect general principles for local activation, polarization, and organization at the cell surface.

Materials and methods

Reagents

Expression plasmids used in this study were gifts from the following sources: PLCδ1-PH-GFP (a gift from E. Tall, SUNY Stony Brook, Stony Brook, NY); cortactin-GFP (Kaksonen et al., 2000; a gift from H.B. Peng, Hong Kong University, Hong Kong, China); synaptojanin (a gift from P. De Camilli, Howard Hughes Medical Institute, Yale University, New Haven, CT); PI5-kinase (a gift from L. Machesky, University of Birmingham, Birmingham, UK); dn-Cdc42 (HA-tag), dn-Rac (myc-tag), dn-Rho (myc-tag) (a gift from A. Hall, University College London, London, UK). The dn-N-WASP construct (deltaWA, lacking the COOH-terminal verprolin, cofilin homology, and acidic domains; Lommel et al., 2001) was a gift from S. Lommel and T.E. Stradal (German Research Center for Biotechnology, Braunschweig, Germany). The raft-targeted double-palmitoylation constructs (GFP or RFP; i.e., tetrameric dsRed) included the first 40 aa of GAP43, as described previously (Laux et al., 2000). DiD (DiD oil; $DiC_{18}(5)$ oil) was purchased from Molecular Probes (working concentration: 10 μM). Inhibitor compounds and growth factors, with their final concentrations, were used as follows: cytochalasin D (2 μM, 30″; Sigma-Aldrich), methyl-β-cyclodextrin (5 mM, 10′-90′; Sigma-Aldrich), U73122 (1 μM, 20′; Sigma-Aldrich), nocodazole (10 μM, 5′), Rp-cAMP (100 μM, 30′; Biolog), Sp-cAMP (50 μM, 30′; Biolog), Wortmannin (100 nM, 1 h; Sigma-Aldrich), PDGF (100 ng/ml, 5′; Sigma-Aldrich), NGF (100 ng/ml, 30″–30′; Invitrogen), Bradykinin (20 mM, 15′; Sigma-Aldrich), Neomycin (10 mM; Sigma-Aldrich). Signal PIP Kit was purchased from Echelon Biosciences. Antibodies and fluorescent reagents were purchased from the following sources: FLAG, anti-vinculin (Sigma-Aldrich); Arp3, IQGAP1 (Santa Cruz Biotechnology, Inc.); cortactin (Upstate Biotechnology); Dynamin II (BD Biosciences); Tyr-tubulin, Ac-tubulin (Sigma-Aldrich); PKA RII (Upstate Biotechnology); myc (Cell Signaling); HA (Roche); Alexa Fluor 488 phalloidin (Molecular Probes); filipin (Fluka). The mAb against PIP2 was a gift from K. Fukami (Tokyo University, Tokyo, Japan), as described previously (Laux et al., 2000). Anti-p75 was a gift from Y. Barde (University of Basel, Basel, Switzerland); the antibody against APC was a gift from I. Naethke (University of Dundee, Dundee, UK). All secondary antibodies were purchased from Molecular Probes.

Cell culture and immunocytochemistry

Cell lines (COS-7, Swiss 3T3, and NIH 3T3, PC12B-GAP43 and PC12B-GAP43(ΔED) (Laux et al., 2000)) were cultured in DME, with 10% FCS and 10% HS (GIBCO BRL). Tissue culture dishes were coated with collagen (30 μg/ml; Sigma-Aldrich). For replating experiments, cells were removed from semi-confluent dishes, and fixed 1 h after replating. For transient transfections, cells were treated with Lipofectamine 2000 reagent (Invitrogen), and analyzed 18–48 h later.

For carrier-mediated application of $PI(4,5)P_2$ to cultured cells, long chain synthetic phospholipids ($PI(4,5)P_2$ di C_{16}, final concentration 300 μM; Echelon Biosciences) were resuspended in 4 mM KCl, 150 mM NaCl and 20 mM Hepes, pH 7.2. Histone carrier H1 was resuspended in the same buffer, at a concentration of 100 μM. Carrier-phospholipid complex was formed by coincubating phospholipid and carrier at RT for 10 min, followed by a10-fold dilution in DME with 10% HS and 5% FCS-DME. Cells were exposed to this $PI(4,5)P_2$-histone complex for 20 min, and then imaged. In control experiments, uptake and lamellipodial accumulation of carrier were verified with a fluorescent reagent ($PI(4,5)P_2$ C_6-NBD, C_{16}; Echelon Biosciences).

To visualize cholesterol and raft markers, cells were fixed for 20 min at 37°C in 4% PFA, 0.4 mM $CaCl_2$, 50 mM sucrose, 100 mM NaH_2PO_4, washed, and then incubated with antibody solution. For $PI(4,5)P_2$ stainings, cells were fixed in 4% PFA in DME with 2 mM EGTA (30′, 37°C), followed by 5 h at 4°C. First antibody incubations were overnight at 4°C, in PBS, 0.2% saponin, 50 mM glycine, 0.1% BSA, 1% FCS. In similar experiments, permeabilization of fixed cells at RT with 0.1% Triton X-100 instead of saponin led to a loss of PHδ1-GFP, raft markers and f-actin signal from most cell surface patches, suggesting that at RT these membrane domains are particularly sensitive to detergent extraction. Images were obtained and processed using a Nikon epifluorescence microscope (100×, oil immersion) and Act-1 software, or with an Olympus confocal microscope (63×, oil) and Fluoview software. All experiments were performed at least five times independently, and representative examples are shown in the figures.

For the analysis of Triton-insoluble fractions, cells were grown to 80% confluency, washed 3× with PBS, and scrapped from the culture dish in 1 ml of 25 mM Tris-Cl, pH 7.5, 150 mM NaCl, 5 mM EDTA, protease inhibitor cocktail (Roche), and 1% Triton X-114. After homogenization (glass homogenizer, 50 strokes), cells were left for 1 h on ice, and centrifuged at 15,000 *g* (15 min, 4°C). Pellet and supernatant were collected separately, equal amounts of protein were loaded on 10% SDS/PAGE gels, and protein contents visualized on immunoblots. In separate experiments, cells were homogenized as described above, homogenates made to 40% sucrose (with an 80% sucrose solution; 2 ml total), and overlaid with 30% sucrose (3 ml), 20% sucrose (3 ml), 10% sucrose (3 ml), and buffer (2 ml). After centrifugation, (70,000 *g*, 20 h, 4°C), a raft band (R) was collected at the 10/20% sucrose interface, and the majority of membranes (M) was collected as a pellet.

Oligonucleotides for RNAi of rat IQGAP1 were 5′-AAGGGTGATAATGCTCACC-3′, and 5′-AATGAGAGACTCACGGCAT-3′ (synthesized by Ambion). Cells were transfected with (or without; mock transfection) 20 nM of siRNA and 4 μl of Lipofectamine 2000 reagent in 35-mm dishes, with 0.9 ml of OptiMEM. After 4 h of incubation at 37°C, cells were switched back to growth medium (10% HS + 5% FCS, DME), and analyzed 48 h later. Transfection efficiencies were 50–60%, and residual IQGAP1 signals were 0–20% of control.

Live imaging

Cells were imaged with a Zeiss Axioskop, a water immersion objective (Achroplan 100×/1.0W; Carl Zeiss MicroImaging, Inc.), filters to reduce fluorescent light, and a digital CCD camera (C4742-95; Hamamatsu), controlled by QED camera plug-in for Power Mac G4 (QED Imaging Inc.). Images were acquired every 10 s, and imaging sessions ranged from 6–20 min. For live imaging, cells were kept at 37°C (heated microscope stage), in Tyroid's imaging buffer (2.68 mM KCl, 0.5 mM $MgCl_2$, 137 mM NaCl, 0.36 mM NaH_2PO_4, 5.5 mM glucose, 1.8 mM $CaCl_2$). For DiD imaging, cells were preincubated in growth medium with 10 μM DiD for 5 min, washed three times with PBS and imaged. Where appropriate (e.g., nonfluorescent transgenes), the expression of transgenes in imaged cells was subsequently verified by immunocytochemistry. In control experiments, cells were reexamined 1–6 h after imaging, and exhibited no obvious signs of phototoxicity (e.g., blebbing).

A confocal microscope (LM 510 meta; Axioplan2; Carl Zeiss MicroImaging, Inc.) was used to acquire live images (512 × 512 resolution; 8-bit images; 63×, NA = 0.95 objective) of double-labeled cells (DiI/PHδ1-GFP; ppRFP/PHδ1-GFP) and for FRAP experiments. An Argon2 laser was used to excite GFP constructs (1% intensity); RFP and DiI constructs: HeNe1 laser (24% intensity). Two-colors acquisition was performed using multi-tracking. Emission filters: BP505-530 (488-nm excitation); LP560 (543-nm excitation). During imaging, cells were kept in a microscope chamber at 37°C. Step sizes for Z-sectioning were 0.5 μm (optical slices <2.3 μm).

Consistent with the notion that PHδ1-GFP predominantly visualizes raft-associated $PI(4,5)P_2$, PHδ1-GFP, and ppgFP constructs yielded comparable results. In control experiments, DiD did not highlight comparable structures associated with ruffling lamellipods in NGF-treated PC12 cells (Video 5), validating the use of PHδ1-GFP and ppGFP to visualize $PI(4,5)P_2$-rich raft patches associated with actin-based motility in living cells.

FRAP analysis

For FRAP measurements, the confocal pinhole was set at 1 Airy unit, and photobleaching was performed using 100 It (Argon2 laser; 100% intensity; rectangular regions of 20–30 × 20–30 pixels). Fluorescence recoveries and bulk photobleaching during the time series were analyzed using LSM software (version 2.5 SP2; Carl Zeiss Microimaging, Inc.). Images were acquired at intervals of 3.4–4.0 s. All intensity values were corrected for bulk photobleaching caused by scanning. For FRAP of raft patches, structures with areas of 0.2–0.5 μm^2 (untreated cells), 1.5–2.5 μm^2 (+NGF), 0.5–1 μm^2 (nocodazole or Rp-cAMP, +NGF), or 3–4 μm^2 (Sp-cAMPS, +NGF) were analyzed.

The comparatively slow FRAP rates of ppGFP at $PI(4,5)P_2$-rich raft patches did not correlate with the relative intensities of the ppGFP signal at the patches.

Quantitative analysis

All data to be compared were acquired with identical camera settings, and images were analyzed quantitatively using Image-Pro 5 software (Media Cybernetics). All isolated cells from randomly selected fields (100− objectives) were analyzed. To compare intensities (arbitrary units) or define threshold values for patches, sets of data were calibrated by setting individual zero (no cells) and background fluorescence values inside cells (fixed cells: 50; PH-GFP: 80). Co-localization of antigen labeling with f-actin or raft markers (GAP43 unless stated otherwise) was assessed using the count/size function, and computing Pearson's correlation coefficients. Thresholds were set to include all clearly defined structures (values of 20–30 above background fluorescence). For Pearson's coefficients to f-actin patches, background values were defined at 120, to restrict the sample to lamellipodial f-actin. Where specified (edge), only structures within 2.5 μm of the cell edge were included. Images of double-labeled cells were then compared electronically. The Pearson's correlation coefficient (1 = highest value, 0 = lowest value) is a measure of the linear association between two variables.

For patch size analysis, all patches within 2.5 × 8 μm masks were analyzed. Where specified (edge), masks were placed with their long axis tangential to cell edge lamellipodia. Patches smaller than 0.2 μm^2 were considered as background, and excluded when deriving values for patch numbers and average patch size. Data from cells derived from 3–5 independent experiments were pooled and medial values per unit area were calculated. To derive labeling intensity ratios, intensities at the brightest patches or lamellipods of a given cell were related to average values at the corresponding structures of the same cell. Average MT to cell edge counts are given per cell, and only include MTs apparently ending at the cell edge (usually with bright tubulin heads).

For the analysis of fluorescent time-lapse recordings, individual cell edge patches were followed for at least 5 min, and data pooled for individual time points after the addition of NGF. Patch boundaries exhibited thresholds of at least 30 U over surrounding background values (a background value of 80 was subtracted from all patch intensity values). Both, edge patch intensity and area values reflect averages at individual patches.

For the analysis of phase-contrast time-lapse recordings, images from individual time frames were aligned, and entire cell edge regions not contacting neighboring cells were analyzed. Occasional cells that did not respond to NGF with lamellipodial motility (<10–15% of total) were excluded from the analysis. Cell outlines from 20-s time intervals were traced and overlaid using fiduciary marks, defining individual "difference cell edge areas" that had either extended or retracted (mean area values). For average motility values, the areas were all summed (irrespective of whether they represented advances or retractions), and normalized to 15-s intervals, and total cell outline lengths (μm/15 s). Average motility values were derived from sets of such comparisons within defined 1-min intervals, as indicated. Net/total motility ratios (100%) were derived by calculating individual net advance or retraction areas (the sum of all advances, minus the sum of all retractions) per unit time and particular cell edge region, and dividing these values by the total value of corresponding advance and retraction areas.

Online supplemental material

The Online supplemental material contains the following data. Fig. S1 shows evidence that cell surface rafts accumulate at motile lamellipods. Fig. S2 shows evidence for stabilization of microtubules at PI(4,5)P2-rich raft patches. Fig. S3 shows evidence that MTs promote raft patch clustering, and contain motility at the cell edge. Fig. S4 shows evidence for the association of APC with cell edge raft patches. Video 1 shows phase-contrast time-lapse recording of PC12 cells in the absence of NGF. Video 2 shows phase-contrast time-lapse recording of NGF-treated PC12 cells. Video 3 shows phase-contrast time-lapse recording of PC12 cell pretreated with cyclodextrin, and then with NGF. Video 4 shows GFP-fluorescence time-lapse recording of NGF-treated PC12 cell expressing PHd1-GFP. Video 5 shows time-lapse recording of NGF-treated PC12 cells labeled with DiD. Video 6 shows GFP-fluorescence time-lapse recording of NGF-treated PC12 cells co-expressing PHd1-GFP and Dn-Cdc42. Video 7 shows phase-contrast time-lapse recording of NGF-treated PC12 cells in the presence of nocodazole. Video 8 shows GFP-fluorescence time-lapse recording of NGF-treated PC12 cells expressing PHd1-GFP in presence of nocodazole. Video 9 shows GFP-fluorescence time-lapse recording of NGF-treated PC12 cells expressing PHd1-GFP in the presence of Sp-cAMP. Video 10 shows GFP-fluorescence time-lapse recording of NGF-treated PC12 cells expressing PHd1-GFP in presence of Rp-cAMP. Online supplemental material is available at http://www.jcb.org/cgi/content/full/jcb.200407058/DC1.

We thank P. De Camilli (New Haven), K. Fukami (Tokyo), S. Lommel and T.E. Stradal (Braunschweig), I. Naethke (Dundee), H.B. Peng (Hong Kong), and E. Tall (Stony Brook) for generously providing precious reagents. We are indebted to T. Laroche (Friedrich Miescher Institut) for precious help with the FRAP experiments. We are grateful to S. Arber (Basel) for valuable comments on the manuscript. The Friedrich Miescher Institut is part of the Novartis Research Foundation.

Submitted: 9 July 2004
Accepted: 2 March 2005

References

Botelho, R.J., M. Teruel, R. Dierckman, R. Anderson, A. Wells, J.D. York, T. Meyer, and S. Grinstein. 2000. Localized biphasic changes in phosphatidylinositol-4,5-bisphosphate at sites of phagocytosis. *J. Cell Biol.* 151: 1353–1367.

Caroni, P. 2001. Actin cytoskeleton regulation through modulation of $PI(4,5)P_2$ rafts. *EMBO J.* 20:4332–4336.

Cremona, O., and P. De Camilli. 2001. Phosphoinositides in membrane traffic at the synapse. *J. Cell Sci.* 114:1041–1052.

del Pozo, M.A., N.B. Alderson, W.B. Kiosses, H.-H. Chiang, R.G.W. Anderson, and M.A. Schwartz. 2004. Integrins regulate Rac targeting by internalization of membrane domains. *Science.* 303:839–842.

Etienne-Manneville, S., and A. Hall. 2002. Rho GTPases in cell biology. *Nature.* 420:629–635.

Etienne-Manneville, S., and A. Hall. 2003. Cdc42 regulates GSK-3β and adenomatous polyposis coli to control cell polarity. *Nature.* 421:753–756.

Fukata, M., T. Watanabe, J. Noritake, M. Nakagawa, M. Yamaga, S. Kuroda, Y. Matsuura, A. Ywamatsu, F. Perez, and K. Kaibuchi. 2002. Rac1 and Cdc42 capture microtubules through IQGAP1 and CLIP-170. *Cell.* 109: 873–885.

Golub, T., S. Wacha, and P. Caroni. 2004. Spatial and temporal control of signaling through lipid rafts. *Curr. Opin. Neurobiol.* 14:542–550.

Gomez-Mouton, C., R.A. Lacalle, E. Mira, S. Jimenez-Baranda, D.F. Barber, A.C. Carrera, C. Martinez-A, and S. Manes. 2004. Dynamic redistribution of raft domains as an organizing platform for signaling during cell chemotaxis. *J. Cell Biol.* 164:759–768.

Gordon-Weeks, P.R. 2004. Microtubules and growth cone function. *J. Neurobiol.* 58:70–83.

Grimmer, S., B. van Deurs, and K. Sandvig. 2002. Membrane ruffling and macropinocytosis in A431 cells require cholesterol. *J. Cell Sci.* 115:2953–2962.

Guirland, C., S. Suzuki, M. Kojima, B. Lu, and J.Q. Zheng. 2004. Lipid rafts mediate chemotropic guidance of nerve growth cones. *Neuron.* 42:51–62.

Gundersen, G.G., E.R. Gomes, and Y. Wen. 2004. Cortical control of microtubule stability and polarization. *Curr. Opin. Cell Biol.* 16:106–112.

Huang, S., L. Lifshitz, V. Patki-Kamath, R. Tuft, K. Fogarty, and M.P. Czech. 2004. Phosphatidylinositol-4,5-bisphosphate-rich plasma membrane patches organize active zones of endocytosis and ruffling in cultured adipocytes. *Mol. Cell. Biol.* 24:9102–9123.

Kaksonen, M., H.B. Peng, and H. Rauvala. 2000. Association of cortactin with dynamic actin in lamellipodia and on endosomal vesicles. *J. Cell Sci.* 113:4421–4426.

Kenworthy, A.K., B.J. Nichols, C.L. Remmert, G.M. Hendrix, M. Kumar, J. Zimmerberg, and J. Lippincott-Schwartz. 2004. Dynamics of putative raft-associated proteins at the cell surface. *J. Cell Biol.* 165:735–746.

Laux, T., K. Fukami, M. Thelen, T. Golub, D. Frey, and P. Caroni. 2000. GAP43, MARCKS, and CAP23 modulate $PI(4,5)P_2$ at plasmalemmal rafts, and regulate cell cortex actin dynamics through a common mechanism. *J. Cell Biol.* 149:1455–1472.

Lommel, S., S. Benesch, K. Rottner, T. Franz, J. Wehland, and R. Kuhn. 2001. Actin pedestal formation by enteropathogenic *Escherichia coli* and intracellular motility of Shigella flexneri are abolished in N-WASP-defective cells. *EMBO Rep.* 2:850–857.

Martin, T.F.J. 2001. $PI(4,5)P_2$ regulation of surface membrane traffic. *Curr. Opin. Cell Biol.* 13:493–499.

McLaughlin, S., J. Wang, A. Gambhir, and D. Murray. 2002. PIP(2) and proteins: interactions, organization, and information flow. *Annu. Rev. Biophys. Biomol. Struct.* 31:151–175.

Mouneimne, G., L. Soon, V. DesMarais, M. Sidani, X. Song, S.C. Yip, M. Ghosh, R. Eddy, J.M. Backer, and J. Condeelis. 2004. Phospholipase C and cofilin are required for carcinoma cell directionality in response to EGF stimulation. *J. Cell Biol.* 166:697–708.

Näthke, I.S., C.L. Adams, P. Polakis, J.H. Sellin, and W.J. Nelson. 1996. The adenomatous polyposis coli tumor suppressor protein localizes to plasma membrane sites involved in active cell migration. *J. Cell Biol.* 134:165–179.

O'Connor, K.L., and A.M. Mercurio. 2001. Protein kinase A regulates Rac and is required for the growth factor-stimulated migration of carcinoma cells. *J. Biol. Chem.* 276:47895–47900.

Palazzo, A.F., C.H. Eng, D.D. Schlaepfer, E.E. Marcantonio, and G.G. Gundersen. 2004. Localized stabilization of microtubules by integrin- and FAK-facilitated Rho signaling. *Science.* 303:836–839.

Pardo, M., and P. Nurse. 2003. Equatorial retention of the contractile actin ring by microtubules during cytokinesis. *Science.* 300:1569–1574.

Pierini, L.M., R.J. Eddy, M. Fuortes, S. Seveau, C. Casulo, and F.R. Maxfield. 2003. Membrane lipid organization is critical for human neutrophil polarization. *J. Biol. Chem.* 278:10831–10841.

Pollard, T.D., and G.G. Borisy. 2003. Cellular motility driven by the assembly and disassembly of actin filaments. *Cell.* 112:453–465.

Raucher, D., T. Stauffer, W. Chen, K. Shen, S. Guo, J.D. York, M.P. Sheetz, and T. Meyer. 2000. Phosphatidylinositol 4,5-bisphosphate functions as a second messenger that regulates cytoskeleton-plasma membrane adhesion. *Cell.* 100:221–228.

Rodriguez, O.C., A.W. Schaefer, C.A. Mandato, P. Forscher, W.M. Bement, and C. Waterman-Storer. 2003. Conserved microtubule-actin interactions in cell movement and morphogenesis. *Nat. Cell Biol.* 5:599–609.

Rozelle, A.L., L.M. Machesky, M. Yamamoto, M.H.E. Driessens, R.H. Insall, M.G. Roth, K. Luby-Phelps, K. Marriott, A. Hall, and H.L. Yin. 2000. Phosphatidylinositol 4,5-bisphosphate induces actin-based movement of raft-enriched vesicles through WASP-Arp2/3. *Curr. Biol.* 10:311–320.

Small, J.V., and I. Kaverina. 2003. Microtubules meet substrate adhesions to arrange cell polarity. *Curr. Opin. Cell Biol.* 15:40–47.

Tall, E.G., I. Spector, S.N. Pentyala, I. Bitter, and M.J. Rebecchi. 2000. Dynamics of phosphatidylinositol 4,5-bisphosphate in actin-rich structures. *Curr. Biol.* 10:743–746.

Weston, C., B. Yee, E. Hod, and J. Prives. 2000. Agrin-induced acetylcholine receptor clustering is mediated by the small guanosine triphosphatases Rac and Cdc42. *J. Cell Biol.* 150:205–212.

Wilson, B.S., S.L. Steinberg, K. Liederman, J.R. Pfeiffer, Z. Surviladze, J. Zhang, L.E. Samelson, L.H. Yang, P.G. Kotula, and J.M. Oliver. 2004. Markers for detergent-resistant lipid rafts occupy distinct and dynamic domains in native membranes. *Mol. Biol. Cell.* 15:2580–2592.

Wu, J.Q., J.R. Kuhn, D.R. Kovar, and T.D. Pollard. 2003. Spatial and temporal pathway for assembly and constriction of the contractile ring in fission yeast cytokinesis. *Dev. Cell.* 5:723–734.

Yamaoka-Tojo, M., M. Ushio-Fukai, L. Hilenski, S.I. Dikalov, Y.E. Chen, T. Tojo, T. Fukai, M. Fujimoto, N.A. Patrushev, N. Wang, et al. 2004. IQGAP1, a novel vascular endothelial growth factor receptor binding protein, is involved in reactive oxygen species-dependent endothelial migration and proliferation. *Circ. Res.* 95:276–283.

Yin, H.L., and P.A. Janmey. 2003. Phosphoinositide regulation of the actin cytoskeleton. *Annu. Rev. Physiol.* 65:761–789.